

# Reconstruction of $\tilde{\tau}_1$ mass at the LHC

**Rashid M. Djilkibaev<sup>1</sup>\*, Rostislav V. Konoplich<sup>1,2</sup>**

<sup>1</sup>Department of Physics, New York University, New York, NY 10003

<sup>2</sup>Manhattan College, Riverdale, New York, NY, 10471

January 2, 2019

## Abstract

The cascade mass reconstruction approach was used for mass reconstruction of the lightest stau produced at the LHC in the cascade decay  $\tilde{g} \rightarrow \tilde{b}b \rightarrow \tilde{\chi}_2^0 bb \rightarrow \tilde{\tau}_1 \tau bb \rightarrow \tilde{\chi}_1^0 \tau \tau bb$ . The stau mass was reconstructed assuming that masses of gluino, bottom squark and two lightest neutralinos were reconstructed in advance.

SUSY data sample sets for the SU3 model point containing 160k events each were generated which corresponded to an integrated luminosity of about  $8\text{fb}^{-1}$  at 14 TeV. These events were passed through the AcerDET detector simulator, which parametrized the response of a generic LHC detector. The mass of the  $\tilde{\tau}_1$  was reconstructed with a precision of about 20% on average.

---

\*Permanent address: Institute for Nuclear Research, 60-th Oct. pr. 7a, Moscow 117312, Russia

# I. Introduction

If supersymmetry exists at an energy scale of  $\sim 1$  TeV, SUSY particles such as gluinos and squarks should be abundantly produced at the LHC. Assuming R-parity conservation, these particles cascade down to the lightest supersymmetric particles (LSPs). A detailed discussion of possible SUSY effects at the LHC is given in [1].

In this paper we consider a mass reconstruction of the lightest stau ( $\tilde{\tau}_1$ ) in the cascade decay

$$\tilde{g} \rightarrow \tilde{b}b \rightarrow \tilde{\chi}_2^0 bb \rightarrow \tilde{\tau}_1 \tau bb \rightarrow \tilde{\chi}_1^0 \tau \tau bb \quad (1)$$

The gluino decay chain (1) is shown in Fig.(1)

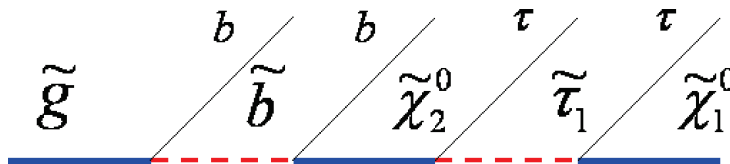


Figure 1: A gluino cascade decay chain.

The study of sleptons and squarks of third generation is of a special interest. Their masses can be very different than that of sparticles of the first and second generation, because of the effects of large Yukawa and soft couplings in the renormalization group equations. Furthermore they can show large mixing in pairs  $(\tilde{t}_L, \tilde{t}_R)$ ,  $(\tilde{b}_L, \tilde{b}_R)$  and  $(\tilde{\tau}_L, \tilde{\tau}_R)$ . The properties of  $\tilde{\tau}_1$  are also important for determination of the dark matter relic density.

The reconstruction of a SUSY event is complicated because of escaping LSPs and many complex and competing decay modes. At present there are two different approaches to SUSY mass reconstruction. The “endpoint method”, which has been widely studied [2] - [9] for the LHC at high integrated luminosity of about  $100 - 300 \text{ fb}^{-1}$ , looks for kinematic endpoints of invariant mass distributions. The second method of SUSY particle mass reconstruction is the “mass relation approach” [10] - [11], based on the mass relation equation which relates SUSY particle masses and measured momenta of detected particles. It was shown in [12] that the “mass relation approach” can be used for luminosities as low as a few  $\text{fb}^{-1}$ .

In this work the cascade mass reconstruction approach [12], that we developed earlier and applied to a different SUSY cascade decay, is used for mass reconstruction of the lightest stau at the LHC energy of 14 TeV with an integrated luminosity of about  $8 \text{ fb}^{-1}$ . The stau mass is reconstructed assuming that the masses of the gluino, bottom squark and two lightest neutralinos were reconstructed in advance. At high integrated luminosity the stau mass could be extracted directly from the endpoint of  $\tau\tau$  invariant mass distribution. However at integrated luminosities below  $10 \text{ fb}^{-1}$  the problem becomes quite challenging because there is no a sharp edge in the  $\tau\tau$  invariant

mass distribution because of escaping neutrinos, a reconstructed stau mass is very sensitive to uncertainties in input parameters (neutralino masses) and there is a high level of SUSY background.

The cascade mass reconstruction approach [12] applied for stau mass reconstruction in this work is based on a consecutive use of the endpoint method, an event filter and a combinatorial mass reconstruction method. The endpoint method is used to get a rough estimate of the stau mass and the corresponding errors. This first estimate of mass is used by an event filter for each event in the data sample to reduce background for the following mass reconstruction step. Finally, the stau mass is reconstructed by a maximization of a combined likelihood function, which depends on all five sparticle masses (gluino, bottom squark, stau and two lightest neutralinos), and is constructed for each possible combination of five events in the data sample.

## II. Simulation

We choose for this study the SU3 model point. This point has a significant production cross section for the chain (1); gluinos and squarks should be produced abundantly at the LHC. The bulk point SU3 is the official benchmark point of the ATLAS collaboration and it is in agreement with the recent precision WMAP data [13]. This model point is described by the set of mSUGRA parameters given in Table (1).

Point	$m_0$	$m_{1/2}$	$A_0$	$\tan\beta$	$\mu$
SU3	100 GeV	300 GeV	-300 GeV	6	$> 0$

Table 1: mSUGRA parameters for the SU3 point.

Assumed theoretical masses of SUSY particles in the cascade (1), the total branching ratio and a cross section generated by ISAJET 7.74 [14] are given in Table (2).

Point	$m_{\tilde{g}}$	$m_{\tilde{b}_1}$	$m_{\tilde{b}_2}$	$m_{\tilde{\chi}_2^0}$	$m_{\tilde{t}\tilde{a}u_1}$	$m_{\tilde{\chi}_1^0}$	BR	$\sigma[\text{pb}]$
SU3	720.16	605.93	642.00	223.27	151.46	118.83	2.71%	19

Table 2: Assumed theoretical masses of sparticles, branching ratio BR and production cross section  $\sigma$  at the SU3 point. Masses are given in GeV.

Branching ratios for the gluino decay chain (1) at the SU3 point are

$$\tilde{g} \xrightarrow{16.6\%} \tilde{b}_1 \xrightarrow{24.1\%} \tilde{\chi}_2^0 \xrightarrow{48.7\%} \tilde{\tau}_1 \xrightarrow{100\%} \tilde{\chi}_1^0 \Rightarrow 1.96\%$$

$$\tilde{g} \xrightarrow{9.2\%} \tilde{b}_2 \xrightarrow{16.6\%} \tilde{\chi}_2^0 \xrightarrow{48.7\%} \tilde{\tau}_1 \xrightarrow{100\%} \tilde{\chi}_1^0 \Rightarrow 0.75\%$$

Monte Carlo simulations of SUSY production at model points were performed by the HERWIG 6.510 event generator [15]. The produced events were passed through the AcerDET detector simulation [16], which parametrized the response of a detector (LHC detector descriptions can be found in [17], [18]). The efficiency for jet reconstruction and labeling was 80%. An additional factor of 50% took into account tau efficiency, which typically corresponded to a rejection factor of about 100 for QCD jets background. Samples of 160k SUSY events were used. This approximately corresponds to  $8 \text{ fb}^{-1}$  of integrated luminosity for the SUSY SU3 point production cross section of 19 pb at 14 TeV. Five different sets of 160k SUSY events were considered to demonstrate the stability and precision of the mass reconstruction approach.

As input parameters for the stau mass reconstruction procedure, hypothetical masses of the gluino, bottom squark and two lightest neutralinos are used. These input masses are assumed to have been reconstructed by the cascade mass reconstruction approach for SUSY data sets corresponding to  $4 \text{ fb}^{-1}$  [12] and are presented in Table 3.

Set	$m_{\tilde{g}}$	$m_{\tilde{b}}$	$m_{\tilde{\chi}_2^0}$	$m_{\tilde{\chi}_1^0}$
1	$701 \pm 57$	$600 \pm 57$	$208 \pm 21$	$98 \pm 22$
2	$712 \pm 55$	$608 \pm 53$	$254 \pm 21$	$143 \pm 20$
3	$664 \pm 78$	$564 \pm 80$	$219 \pm 24$	$109 \pm 23$
4	$767 \pm 62$	$649 \pm 65$	$258 \pm 35$	$148 \pm 34$
5	$655 \pm 45$	$545 \pm 47$	$208 \pm 21$	$96 \pm 20$

Table 3: Reconstructed SUSY particle masses and reconstruction errors for five data sample sets.

In order to isolate the chain (1) the following cuts were applied:

- two jets tagged as  $\tau$  with opposite charge satisfying transverse momentum cuts  $p_T > 30 \text{ GeV}$  and  $p_T > 25 \text{ GeV}$
- two b-tagged jets;
- at least four jets, satisfying  $p_{T1} > 100 \text{ GeV}$ ,  $p_{T2} > 50 \text{ GeV}$ ,  $p_{T3} > 50 \text{ GeV}$ ,  $p_{T4} > 50 \text{ GeV}$ ;
- $M_{eff} > 500 \text{ GeV}$  and  $E_T^{miss} > 0.2 M_{eff}$ , where  $E_T^{miss}$  is the event's missing transverse energy and  $M_{eff}$  is the scalar sum of the missing transverse energy and the transverse momenta of the four hardest jets;
- invariant mass of  $\tau$ -tagged jets satisfying  $10 \text{ GeV} < M_{\tau\tau} < 300 \text{ GeV}$ .

Note that at the first stage of the reconstruction procedure, the stau mass is estimated by considering the chain  $\tilde{q}_L \rightarrow \tilde{\chi}_2^0 q \rightarrow \tilde{\tau} \tau_2 q \rightarrow \tilde{\chi}_1^0 \tau \tau q$  with the same cuts as mentioned above except requiring b-tagged jets.

It was shown in [6] that the Standard Model processes are suppressed significantly by the above requirements on  $\tau$ -tagged jets. The Standard Model dominant backgrounds surviving the hard cuts are  $Z + \text{jets}$  and  $t\bar{t}$  production, where both  $W$ 's decay leptonically into a  $b\bar{b}l\bar{l}$  state. This background was estimated to be 1/10 of the SUSY backgrounds [6]. The  $t\bar{t}$  background can be reduced to about 2% by applying the event filter procedure of the cascade mass reconstruction approach [12]. Thus, the remaining Standard Model contribution is negligible in comparison with that of SUSY backgrounds, and therefore Standard Model background is not included in the following analysis, the SUSY background is about three times the signal rate.

Table (4) shows the number of signal events and SUSY background events for the SU3 model point after cuts were applied to the five sets of 160k SUSY events. The dominant SUSY background consists of  $\tau^+$  and  $\tau^-$  produced in two different decay chains. The classification of events as signal and SUSY background is based on simulated truth information. The SUSY background to the process (1) is significant. It follows from Table (4) that for the SU3 point the number of SUSY background events is a factor 3 greater than the number of signal events.

Set	Total	Signal	SUSY Backg.	Ratio
1	199	47	152	4.2
2	212	56	156	3.8
3	216	53	163	4.1
4	216	48	168	4.5
5	229	65	164	3.5
1-5	1072	269	803	4.0

Table 4: The number of signal and SUSY background events after cuts applied to 160k SUSY events. Ratio = (Signal+Background)/Signal. Row 1-5 shows the number of events for five sets combined.

### III. Preliminary estimate of stau mass by the endpoint method with low statistics

The endpoint method has been widely used to determine masses of SUSY particles [4], in particular it has been applied to the decay chain [6], [19] - [21]

$$\tilde{q}_L \rightarrow \tilde{\chi}_2^0 q \rightarrow \tilde{\tau}_1 \tau q \rightarrow \tilde{\chi}_1^0 \tau \tau q \quad (2)$$

which is a subprocess of the cascade (1) if one considers  $\tilde{q}_L$  instead of  $\tilde{b}$ .

Fig. (2) shows the  $\tau\tau$  invariant mass distribution for Set 1 of 160k events at the SU3 point after application of the kinematic cuts and after subtraction

of same sign  $\tau$ -tagged (background) jets was performed. This allowed to reduce background because in background processes positive and negative jets are mostly uncorrelated.

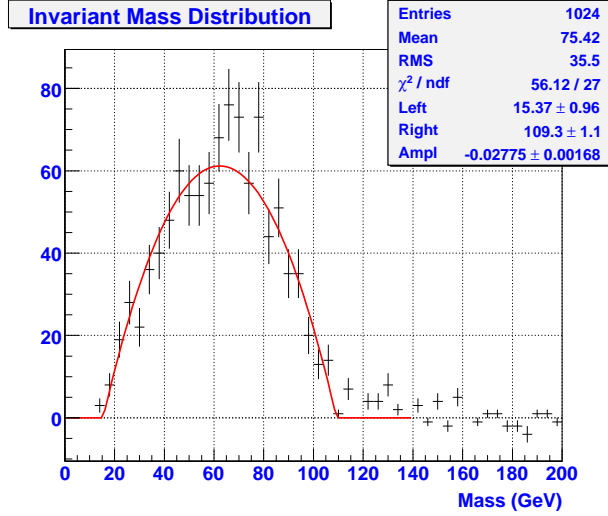


Figure 2: Invariant mass distribution of  $\tau$ -tagged jets for Set 1.

The distribution in Fig. (2) does not have a sharp edge because of undetected neutrino energy in tau-decays but the end-point is clearly seen at about 109 GeV and can be reconstructed.

To extract endpoints from the  $\tau\tau$  invariant mass distribution a fit to this distribution was performed using a parabola plus a straight line that matched the parabola.

The results of the fit for the five data sets are shown in Table (5).

	Set 1	Set 2	Set 3	Set 4	Set 5
<i>endpoint</i>	$109.3 \pm 1.1$	$105.0 \pm 1.0$	$104.0 \pm 0.7$	$108.5 \pm 1.0$	$106.8 \pm 0.6$

Table 5: Endpoints determined from fitting of  $\tau\tau$ -edges.

These results have to be compared with the theoretical endpoint of 101.7 GeV for the SU3 point. The fit was performed by MINUIT [22] which gave errors presented in Table (5). These uncertainties are small because of a specific form of the fit function. More conservative estimates of uncertainties [6], [20] are about 4 GeV but in our case this contribution is not important because the most significant uncertainties come from 20% uncertainties in sparticle masses.

Once endpoints are found the stau mass can be preliminary estimated from the analytical expression for the  $\tau\tau$  endpoint

$$m_{\tau\tau}^2 = (\tilde{\xi} - \tilde{\tau})(\tilde{\tau} - \tilde{\chi})/\tilde{\tau} \quad (3)$$

The following notations are used for masses  $\tilde{\chi} = m_{\tilde{\chi}_1^0}^2$ ,  $\tilde{\tau} = m_{\tilde{\tau}_1}^2$ ,  $\tilde{\xi} = m_{\tilde{\chi}_2^0}^2$ .

The results of the fit for preliminary stau mass estimates and their errors based on found endpoints, edge reconstruction errors, sparticle masses and their errors are summarized in Table (6).

$\tilde{\tau}_1$	Set 1	Set 2	Set 3	Set 4	Set 5
solution 1	149±135	209±48	174±56	205±151	159±51
solution 2	137±137	173±47	138±54	187±150	125±50

Table 6: Stau masses preliminary determined from fitting of  $\tau\tau$ -edges. For each set two stau mass solutions are given.

It is seen from Table (6) that uncertainties of stau mass reconstruction are very large and additional steps in stau mass reconstruction are required.

Eq.(3) gives two solutions for stau mass. Because we use these masses as a rough estimate for more precise procedures described below in the following an average of these two solutions is used as an estimate for the stau mass. Final results are not sensitive to this approximation. In particular, a good estimate for the stau mass at this stage would be just an average of two lightest neutralino masses.

## IV. Background suppression

As a second step of stau mass reconstruction an event filter is used to suppress background before the final fit. At the event filter stage we assume that three light SUSY particle masses ( $\tilde{\chi}_2^0$ ,  $\tilde{\tau}_1$ ,  $\tilde{\chi}_1^0$ ) are fixed. The mass of  $\tilde{\tau}_1$  is taken as the preliminary mass found by the endpoint method in the previous chapter. Neutralino masses are taken from Table 3. Gluino and sbottom masses are assumed to be distributed uniformly in the range  $m_{\tilde{g}} \pm 2\sigma$ ,  $m_{\tilde{b}} \pm 2\sigma$  where masses and errors are given in Table 3.

The event filter procedure is based on minimization for each event of the function

$$\chi^2(m_{\tilde{g}}, m_{\tilde{b}}) = \sum_{i=1}^4 \frac{(p_i^{event} - p_i^{meas})^2}{\sigma_i^2} + \lambda f(\vec{m}, \vec{p}) \quad (4)$$

where index i runs over two b-quarks and two taus and labels the measured absolute momenta  $p_i^{meas}$ , the uncertainties  $\sigma_i$  in their measurement, and the event true absolute momenta  $p_i^{event}$ . The approximate function (4) takes into account only uncertainties in tau and b-jet energy measurements. Note that positions of each of two b-jets and of each of two taus in the decay chain (1) are unknown. It is quite simple to resolve the b-jets assignment because usually (about 96% of the time) the b-jet with higher  $p_T$  originates from the  $\tilde{b}$ -quark decay. Therefore, for each event we assume that the b-jet

with higher  $p_T$  originates from the  $\tilde{b}$ -quark decay. Taus with higher  $p_T$  (after cuts) are produced in both vertices with comparable probabilities. In this work it is assumed that taus with higher  $p_T$  originate from  $\tilde{\chi}_2$  decay. We use the following parametrization for  $\sigma_i$  in equation (4): for b-jets and tau-jets  $\sigma/E = 0.5/\sqrt{E(GeV)} \oplus 0.03$ . The Lagrange multiplier  $\lambda$  in Eq.(4) takes into account the mass relation constraint  $f(\vec{m}, \vec{p})$  [10] - [12] which relates masses and momenta of particles in the chain (1).

For signal events, the event likelihood distribution has a maximum in the region of the  $(\tilde{g}, \tilde{b})$  mass plane correlated with the true masses of  $\tilde{g}$  and  $\tilde{b}$ . Thus signal events should give a peak in the region of true masses. For background events there is no strong correlation of maximum likelihood distribution with true  $(\tilde{g}, \tilde{b})$  masses. Therefore if we chose arbitrary a point in the  $(\tilde{g}, \tilde{b})$  mass plane in the range  $m_{\tilde{g}} \pm 2\sigma, m_{\tilde{b}} \pm 2\sigma$   $\chi^2$  reaches its minimum in this region with much higher probability for a signal event than for a background one. For each event,  $10^5$  points are generated randomly in the mass plane range  $m_{\tilde{g}} \pm 2\sigma, m_{\tilde{b}} \pm 2\sigma$  and the  $\chi^2$  is calculated. If  $\chi^2 < 10$  in at least 1000 points this event is considered as a signal candidate and it is retained for the subsequent analysis.

After the application of the event filter the ratio of background events to signal events is reduced approximately by a factor 1.5 as can be seen from Table 7. The contribution of the combinatorial background is given approximately by  $((\text{Signal}+\text{Background})/\text{Signal})^5$ , corresponding to five event combinations required at the last step of mass reconstruction, and is therefore significantly suppressed. The suppression factor varies from 5 to 10. Note that any five event combination including at least one background event is considered as a background.

Set	Total Number	Signal Events	SUSY Backg.	Ratio	Suppression Factor
1	199/98	47/33	152/65	4.2/3.0	5
2	212/118	56/49	156/69	3.8/2.4	10
3	216/116	53/39	163/77	4.1/3.0	5
4	216/114	48/37	168/77	4.5/3.1	6
5	229/124	65/55	164/69	3.5/2.3	8
1-5	1072/570	269/213	803/357	4.0/2.7	7

Table 7: The number of signal and background events before/after an application of event filter to 160k SUSY events. The last row shows the sum over all five sets. Ratio = (Signal+Background)/Signal. The last column gives approximately a suppression factor (Ratio<sup>5</sup> before to Ratio<sup>5</sup> after) for five event background combinations.

## V. Stau mass reconstruction

As a third step a combinatorial procedure [12] is used for the final stau mass reconstruction. It is applied only to the events that pass the event filter. At the final stage of mass reconstruction when the physical background has already been reduced, we will consider all possible five event combinations from the event sample.

SUSY particle masses are reconstructed by a search for a maximum of a combined likelihood function constructed for each possible combination of five events in the data sample.

The  $\chi^2$  function for an event is defined by

$$\chi_{event}^2 = \sum_{i=1}^4 \frac{(p_i^{event} - p_i^{meas})^2}{\sigma_i^2} + \sum_{n=1}^5 \frac{(m_n^{event} - m_n)^2}{\sigma_n^2} + \lambda_1 f + \lambda_2 f^{ll} . \quad (5)$$

where the first term takes into account deviations of measured momenta of b-jets and tau-jets from the true ones. The second term takes into account that the masses of sparticles vary from event to event as approximated by a Gaussian of width  $\sigma_n$  instead a Breit-Wigner distribution. In Eq.(5) the mass relation and  $\tau\tau$  edge constraints are taking into account by Lagrange multipliers  $\lambda_1, \lambda_2$ . Standard deviations corresponding to the mass widths are taking to be 15 GeV for the gluino, 5 GeV for bottom squark and 1 GeV for light masses. The first two numbers are comparable with theoretical widths for heavy SUSY particles. The last number takes into account the fact that light SUSY particles are quite narrow or stable. We note that the results of the mass reconstruction are not strongly sensitive to the actual values of sparticle widths.

At this step it is assumed that the starting distributions of the heavy masses are uniform in the range: mean value  $\pm 2\sigma$ , where the mean values and standard deviations are given in Table 3. For the three light masses a Gaussian distribution is assumed with mean values and standard deviations found by the endpoint technique as given in Table 6. The MINUIT code is used to search for the minimum of the  $\chi^2$  function for five event set with five mass parameters.

The reconstructed SUSY particle mass distribution and a result of fitting this distribution by a Gaussian are presented in Fig.3 for Set 1. As can be seen in this figure, the reconstructed mass distribution is well described by a Gaussian except for small tails. The mean values of the Gaussian fit are the reconstructed particle masses.

Final results of this mass reconstruction approach are presented for five data sample sets of 160k events each in Table 8.

It follows from Table 8 that reconstruction errors after the final step are significantly reduced in comparison with preliminary estimates 3 obtained by end-point method.

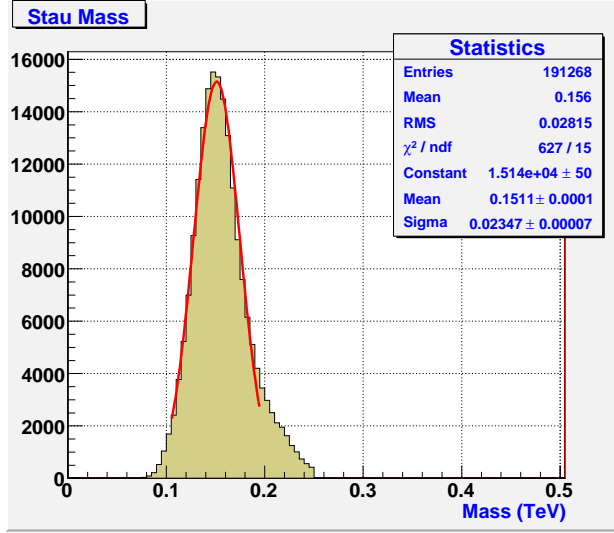


Figure 3: A reconstructed stau mass distribution for Set 1, including SUSY background with integrated luminosity  $8 \text{ fb}^{-1}$ . The line is a result of Gaussian fit.

Particle	Set 1	Set 2	Set 3	Set 4	Set 5
$\tilde{\tau}_1$	$154 \pm 24$	$192 \pm 23$	$168 \pm 25$	$202 \pm 29$	$150 \pm 22$

Table 8: Reconstructed stau masses and reconstruction errors for five data sample sets of 160k events each.

In order to illustrate a spread in reconstructed masses the results of Table 8 are also shown in a form of ideogram [23] in Fig.4 for the five data sample sets. Each reconstructed mass in an ideogram is represented by a Gaussian with a central value  $m_i$ , error  $\sigma_i$  and area proportional to  $1/\sigma_i$ . The solid curve is a sum of these Gaussians.

The Gaussian form of the ideogram and relatively small shift of peak positions with respect to theoretical masses demonstrate the self-consistency of stau mass reconstruction approach.

## IX. Conclusion

We applied the cascade mass reconstruction approach developed in [12] to reconstruction of  $\tilde{\tau}_1$  mass at the LHC with a low integrated luminosity of about  $8 \text{ fb}^{-1}$  at 14 TeV. This luminosity can be reached in the early stage of LHC operation. At low integrated luminosity stau mass reconstruction is complicated because escaping neutrinos modify the edge of the  $\tau\tau$  invariant mass distribution, reconstructed stau mass is very sensitive to uncertainties in input parameters (neutralino masses) and the level of SUSY background is high.

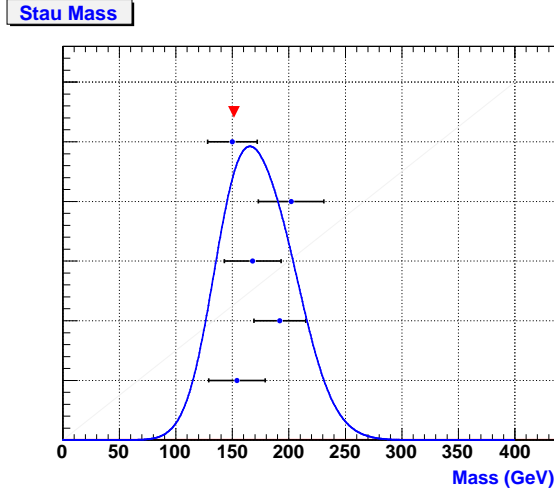


Figure 4: An ideogram of reconstructed stau masses, including SUSY background for five data sample sets with integrated luminosity  $8 \text{ fb}^{-1}$ . The triangle marker gives the position of the SU3 theoretical mass. Points with error bars correspond to five data sample sets.

Our approach to the stau mass reconstruction was based on a consecutive use of the endpoint method, an event filter and a combinatorial mass reconstruction method.

The endpoint method allows preliminary estimate of  $\tilde{\tau}_1$  mass by assuming that sparticle masses required as input parameters for this procedure are known from the same experiment with a precision of about 10% for heavy sparticles (such as gluino and bottom squark) and about 20% for the two lightest neutralinos. In this work these input masses were obtained by the cascade mass reconstruction approach [12]. At high integrated luminosity of  $100 - 300 \text{ fb}^{-1}$  they could be found by using one of techniques proposed in [2] - [11].

The stau mass was reconstructed with a precision of about 20%

## Acknowledgments

The authors thank K.Cranmer, M.Ibe, A.Mincer and P.Nemethy for interesting discussions and useful suggestions. This work has been supported by the National Science Foundation under grants PHY 0428662, PHY 0514425 and PHY 0629419.

## References

- [1] The ATLAS Collaboration, G.Aad et.al., arXiv:0901.0512 (2009).
- [2] H.Baer, K.Hagiwara and X.Tata, Phys.Rev.**D35**(1987)1598;  
H.Baer, D.D.Karatas and X.Tata, Phys.Rev.**D42**(1990)2259;  
H.Baer, C.Kao and X.Tata, Phys.Rev.**D48**(1993)5175;  
H.Baer, C.Chen, F.Paige and X.Tata, Phys.Rev.**D50**(1994)4508.
- [3] S.Abdullin et al. [CMS Collaboration], J.Phys.**G28**(2002)469.
- [4] I.Hinchliffe et al., Phys.Rev.**D55**(1997)5520;  
I.Hinchliffe and F.E.Paige, Phys.Rev.**D61**(2000)095011;  
H.Bachacou, I.Hinchliffe and F.E.Paige, Phys.Rev.**D62**(2000)015009.
- [5] B.C.Allanach, C.G.Lester, M.A.Parker and B.R.Webber, JHEP**0009**  
(2000)004.
- [6] B.K.Gjelsten et al., ATLAS internal note ATL-PHYS-2004-007(2004), published in G.Weiglein et al. [LHC/LC Study group], arXiv:hep-ph/0410364.
- [7] B.K.Gjelsten, D.J.Miller and P.Osland, JHEP**12**(2004)003.
- [8] B.K.Gjelsten, D.J.Miller and P.Osland, JHEP**0506**(2005)015.
- [9] C.G.Lester, M.A.Parker and M.J.White, JHEP**0601**(2006)080.
- [10] M.M.Nojiri, G.Polesello and D.R.Tovey, arXiv:hep-ph/0312317.
- [11] K.Kawagoe, M.M.Nojiri and G.Polesello, Phys.Rev.**D71**(2005)035008.
- [12] R.M.Djilkibaev and R.V.Konoplich, JHEP **0808**(2008)036.
- [13] D.N.Spergel et al., ApJS**170**(2007)377.
- [14] F.E.Paige, D.Protopopescu, H.Baer and X.Tata, arXiv:hep-ph/0312045.
- [15] G.Marchesini et al., Comput.Phys.Commun.**67**(1992)465; G.Corcella et al., JHEP**0101**(2001)010; S.Moretti et al., JHEP**0204**(2002)028.
- [16] E.Richter-Was, arXiv:hep-ph/0207355.
- [17] The ATLAS Collaboration, G.Aad et.al., JINST **3**(2008)S08003.
- [18] The CMS Collaboration, S Chatrchyan et.al., JINST **3**(2008)S08004.
- [19] M.Ibe and R.Kitano, arXiv:0712.3300 (2007).
- [20] K.Desch, T.Nattermann, P.Wienemann and C.Zendler, ATL-PHYS-INT-2008-08.

- [21] T.Nattermann, K.Desch, P.Wienemann and C.Zendler, JHEP **0904**(2009)057.
- [22] F.James and M.Roos, Comput.Phys.Commun.**10**(1975)343.
- [23] Particle Data Group, C.Amsler et al., Phys.Lett. **B667**(2008)1.